Carbonates and Evaporites (2019) 34:441–459
https://doi.org/10.1007/s13146-018-0477-3

ORIGINAL ARTICLE

Depositional and geochemical characteristics of geomorphologically controlled recent tufa deposits on the Göksü River in Yerköprü (Konya, southern Turkey)

Arif Delikan[1] · **Mehmet Mert**[2]

Accepted: 27 September 2018 / Published online: 6 October 2018

Abstract
Recent tufa deposition has been taking place on a 500 m-long natural bridge on the Göksu River in the Yerköprü region, southern Konya, Turkey. The Karasu spring arises from the Karasu normal fault, flows over this natural bridge and drops down from the end of the bridge, forming a spectacular waterfall. There is a dense CO_2 degassing from this water and the $H_2CO_3^{-1}$ content is 506,3 mg/L at the orifice and 549 mg/L on the waterfall, but it drops almost to half at the bottom of the waterfall. The field observation and chemical data showed that the deposition of the studied tufa was related only to the water derived from the Karasu spring. At the active waterfall area, tufa deposition takes place on the cascade, in small and large ponds and in channels. People living in the area build canals for irrigation and milling purposes, which cause the spreading of tufa deposits to other than the main course of the Karasu spring water. The most common types of facies are the different phytotherm facies, but stromatolitic, micritic and phytoclastic facies are also present to a lesser amount. The $\delta^{13}C$ content of the tufa deposits ranges from 1,6 to −3,3 and $\delta^{18}O$ contents from −9,6 to −11,5. The higher $\delta^{13}C$ values of the Yerköprü tufa deposits indicate that the carbonate-rich water of the Karasu spring originated from a carbonate aquifer. The isotopic values of the studied tufa samples are similar to those of travertine, but the Karasu water is interpreted as cold water. Therefore, it may be considered as "travitufa".

Keywords Tufa · Travitufa · Yerköprü · Waterfall · Karasu spring · Sinkhole

Introduction

Tufa is found as common continental carbonate deposits in a wide range of environmental depositional, climatic, and tectonic settings throughout the world (Henning et al. 1983; Magnin et al. 1991; Baker et al. 1993; Ford and Pedley 1996; Pedley et al. 1996; Guo and Riding 1998; Hancock et al. 1999; Arenas et al. 2000; Glover and Robertson 2003; Martìn-Algarra et al. 2003; Andrews 2006; Ozkul et al. 2010; Brasier et al. 2011; Domínguez-Villar et al. 2011; Kosun 2012; Capezzuoli et al. 2014; Özkul et al. 2014; Henchiri 2014a; Della Porta 2015). Tufa is considered to be subaerial deposits produced from ambient cool waters and contains the remains of micro- and macrophytes, gastropods and bivalves and bacteria (Pentecost and Viles 1994; Pedley et al. 2003; Andrews 2006; Ozkul et al. 2010). It is a common continental carbonate deposit in the Holocene and present-day depositional systems of Eastern Europe and the Mediterranean region (Pedley 1990; Ford and Pedley 1996; Guo and Riding 1998; Arenas et al. 2000; Andrews 2006; Ozkul et al. 2010; Capezzuoli et al. 2014; Arenas et al. 2014; Orhan and Kalan 2015; Toker 2017; Pla-Pueyo et al. 2017; Sancho et al. 2015; Karaisaoglu and Orhan 2018; Pisciotta et al.2018). Recently, tufa sediments have been classified by using parameters such as the type of encrusting of the macrophytes, carbonate buildup and the oncolites (Arenas et al. 2000, 2007, Arenas-Abad et al. 2010; Sanders et al. 2011; Henchiri 2014b; Orhan and Kalan 2015; Toker 2017; Pla-Pueyo et al. 2017). Tufa generally contains low-Mg calcite and its deposition is related to the biogenic and physicochemical processes. The textures of the tufa deposits are controlled by the climatic and environmental conditions

✉ Arif Delikan
adeli@selcuk.edu.tr

[1] Department of Geological Engineering, Konya Technical University, Konya, Turkey

[2] DSI the 4. Regional Directorate Konya, Konya, Turkey

(Pedley 1990; Guo and Riding 1999; Brasier et al. 2011; Peng and Jones 2013; Richter et al. 2015).

The purpose of this paper is to describe and interpret the depositional and geochemical characteristics of tufa facies in an active tufa deposition site in the Yerköprü area (South of Konya, Turkey) in terms of sedimentological and stable isotopic data.

Geological setting

The study area is located south of Konya (Turkey) within the central Tauride (Fig. 1), which is highly folded and faulted. The climate in the study area is continental, with cold and snowy winters, and hot and dry summers.

A rare geological structure known as natural bridge or tufa/travertine bridge is present in the Yerköprü area (Figs. 1 and 2). The Yerköprü tufa deposition took place in relation to this natural bridge. The recent Yerköprü tufa sediment was deposited with angular unconformity on the Aladağ terrace tufa (~90–350 ka, Delikan et al. 2017; Fig. 3f), the Permian carbonate rocks (Taşkent formation) and Triassic meta-olistostrome (Zindancık meta-olistostrome).

There are two dip slip normal faults which are parallel to each other on both sides of the Göksü valley: the Yerköprü fault dipping to the south on the north side of the valley and the Karasu fault dipping to the north on the south side of valley (Fig. 1; Delikan and Mert 2014). These faults were developed as steps. The Göksü River flows in the graben between these two faults. At the Yerköprü area, it flows about 500 m beneath an old tufa block fallen from the Göksü valley (Figs. 2 and 4c, d). Besides this, the Karasu spring discharging from the Karasu fault on the south-west part of the tufa deposition area flows over an old tufa block, forming a natural bridge. Bicarbonate-rich water of the Karasu spring drops over a 20-m-high waterfall and mixes with the Göksu River beneath the waterfall (Figs. 2, 3c and 4b, d).

Materials and methods

During the field observations, the lithofacies and their relation were determined, and 78 samples were collected for lithological and geochemical analysis ($\delta^{18}O$ and $\delta^{13}C$ stable isotope, major and trace elements). Samples were collected systematically from places where the tufa sequence was thick. Also, random sampling was realized from different lithologies (in 2013 and 2014). 15 water samples were collected on April 4, 2013 and analyzed with Dionex ICS-1000 in the Water Control Analysis Laboratory of State Hydraulic Works of Turkey. Thin sections and acetate peels from samples were prepared for determining the petrographic and sedimentological characteristics of different facies.

Stable isotope (oxygen and carbon) analyses of 19 carbonate powder samples were performed at the Institute for Geological and Geochemical Research, Hungarian Academy of Sciences, Budapest, Hungary, using an automated carbonate preparation device (Gasbench II) and a Thermo Fisher Scientific Delta Plus XP continuous flow mass spectrometer. Standardization was conducted using laboratory calcite standards calibrated against the NBS 18 and NBS 19 standards. All samples were measured at least in duplicate and the mean values expressed in the conventional δ notation in parts per thousand (‰) on the V-PDB scale (δ13C, δ18O) and VSMOW scale (δ18O). Reproducibility was better than ± 0.1‰ for δ13C and δ18O values of carbonates.

The mineralogical composition of representative samples was determined by Bruker-D8/Advance/X-ray diffraction (XRD) and Zeiss Evo/Ls10-Scanning Electron Microscope (SEM) methods at ILTEK laboratory in Selçuk University.

Chemical analysis (major oxide, trace and rare earth element contents) of ten samples was performed at the ACME analytical laboratories (Vancouver, British Columbia, Canada) by inductively coupled plasma emission and mass spectrometry (ICP-ES–MS) devices.

Results

Facies characteristics

Tufa sediments, which were actively deposited in the Yerköprü area, were defined by following the classification of Pedley (1990), Ford and Pedley (1996), Arenas et al. (2000) and Vazquez-Urbez et al. (2012), based on the field observations and sedimentological and textural characteristics of tufa deposits. Four different lithofacies were determined in the Yerköprü area (Table 1). These facies are the following.

Phytotherm framestone tufa facies

Description

This facies is the most common sediment in the study area and reaches up to 18 m of thickness. It is characterized by encrusted macrophytes (Lmp), bryophytes (Lbr), coated vertical roots, branches and trunks (Lvs) (Figs. 3a, b and 4e, f) and leaf fossils and is highly porous. Concentric layers comprising alternate coarse sparry calcite and micritic layers are common (Fig. 5a, b). The space between encrusted roots is filled with micrite. This facies starts with the formation of crust by water flowing over the branches, roots and plants, such as *Adiantum capillus-veneris* hanging from the slopes (Figs. 3, 6a, b and 7b–d). At the space behind this facies, speleothems were formed by seeping water. The

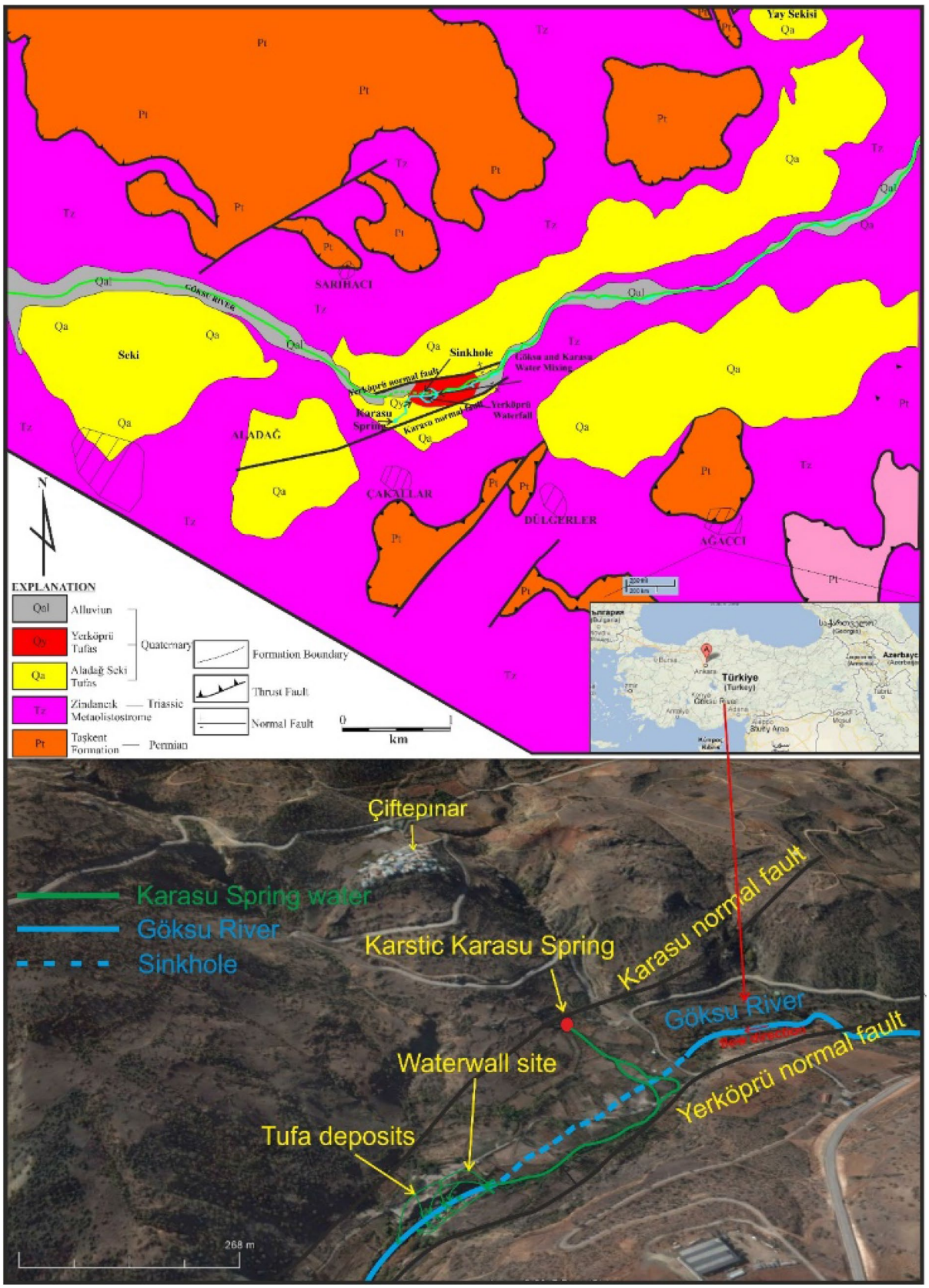

Fig. 1 Geological map of the study area (Delikan and Mert 2014)

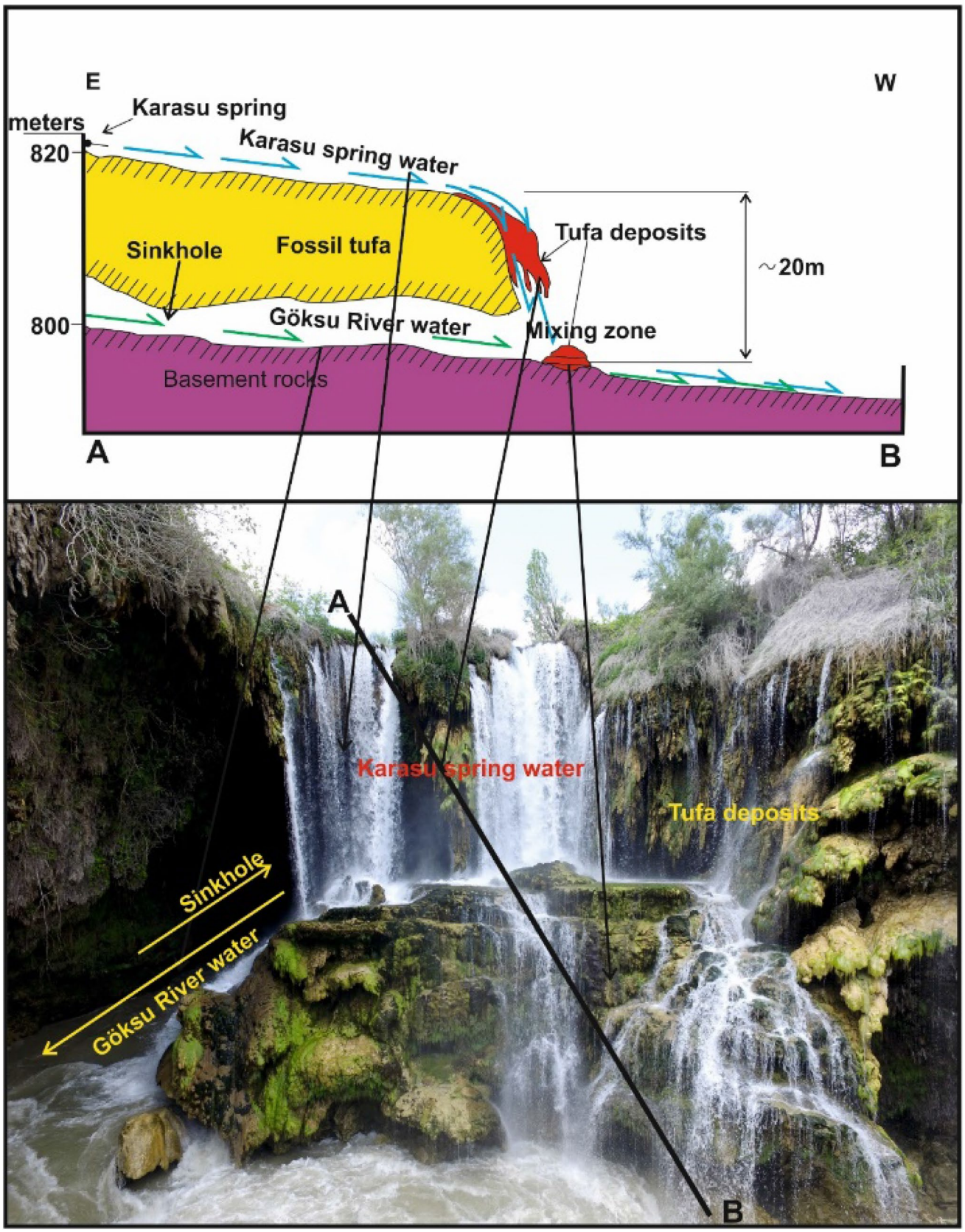

Fig. 2 Field view of the Yerköprü waterfall. The Karasu spring water flow down from the cliff and mixes with the Göksu River flowing beneath the natural bridge

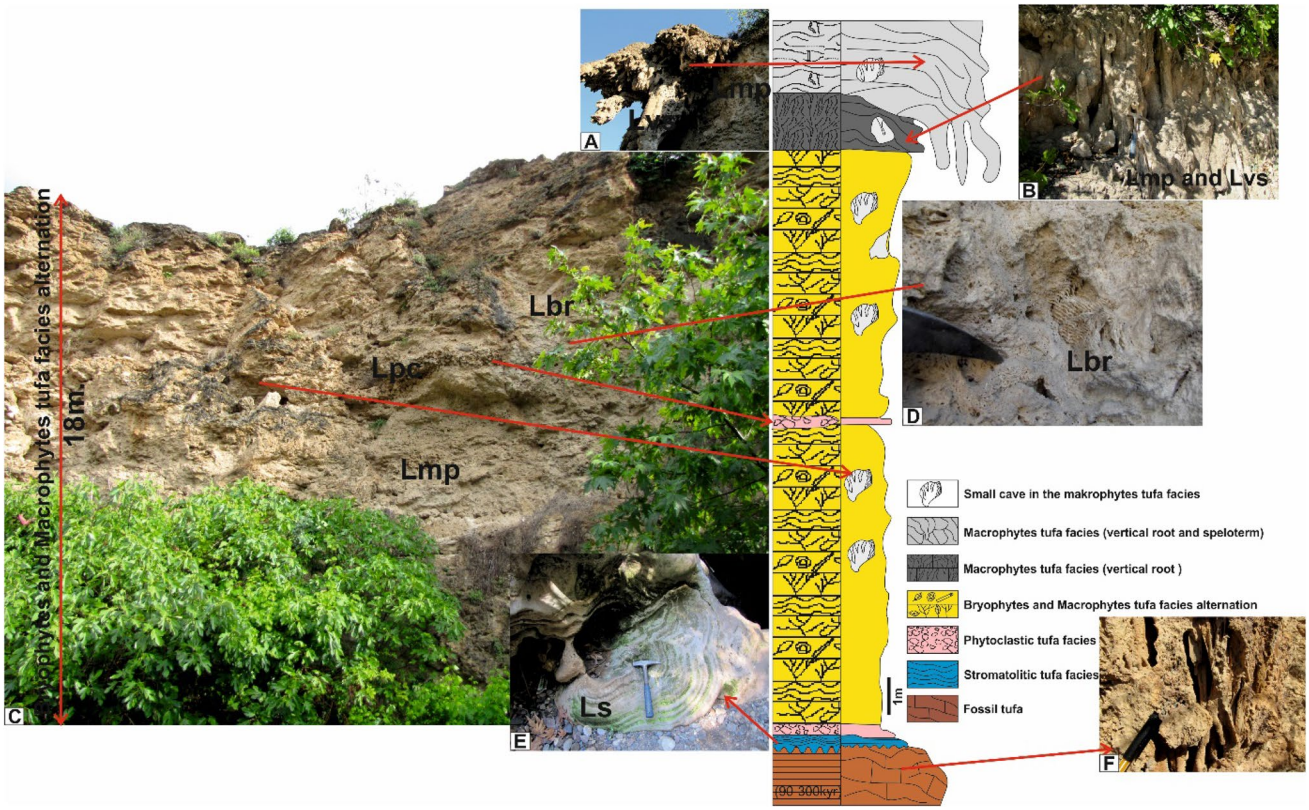

Fig. 3 Measured stratigraphic section and field pictures of different facies. **a** Vertical stems (Lvs) and macrophytes (Lmp), developed at the cascade setting. **b** Vertical stems (Lvs) and macrophytes (Lmp) facies resulted from coating solely tree and plant roots. **c** Approximately, 18 m-thick sequence of intercalated macrophytes (Lmp) and bryophytes (Lbr) tufa facies and phytoclastic tufa facies (Lpc) resulted from flooding. **d** Detailed appearance of the bryophytes tufa facies. **e** Stromatolitic tufa facies (Ls) observed generally at the bottom part of the sequence. **f** The fossil tufa formed by phytotherm tufa facies unconformably underlying the recent tufa deposits

encrusted macrophytes are generally overlain by encrusted bryophytes, which have been repeated several times through tufa sequences (Figs. 3, 7a and 8g, h).

Interpretation

In modern and recent tufa environments, bryophytes develop along the waterfalls, barriers and in water-splash areas beside active channels and pools (Pedley 1990; Ford and Pedley 1996; Arenas et al. 2000; Pentecost 2005¸ Arenas et al. 2007, 2014). Macrophytes tufa facies (Lmp) are generally deposited at the slopes having dense roots and plants and high energy condition. Deposition starts with crust formation around the plants while the water flow is turbulent. After flooding, ponds were formed on the flatness around the waterfall. During these periods, the terrestrial algae growing on the branches and in the pond bring about the development of bryophytic tufa under both turbulent and stagnant conditions (Figs. 5c, 7e, f). *Adiantum capillus-veneris* and the trunk and roots of plants cause the formation of vertical stem tufa (Fig. 6).

Boundstone tufa facies (stromatolitic tufa facies—Ls)

Description

This facies is one of the common facies among the tufa deposits. It is represented by 5 cm to 30 cm thick intercalated light and dark laminae and occurs as domes and columns, planar laminae and slightly crenulated forms (Figs. 3e, 5d and 7h, i). Bedding is generally undulated and comprises hemispheric and kidney-shaped structures. Stromatolitic tufa was observed in the water course channels of the Karasu spring and watermill canals. About 5-m-high wall of stromatolitic tufa was formed in the watermill canals (Fig. 7g). Stromatolitic tufa facies laterally grades into phytotherm framestone facies, as seen in other places (Pedley 2009; Ozkul et al. 2010; Vazquez-Urbez et al. 2012).

Interpretation

Stromatolites may have developed under low energy condition in shallow ponded areas and partially isolated fluvial

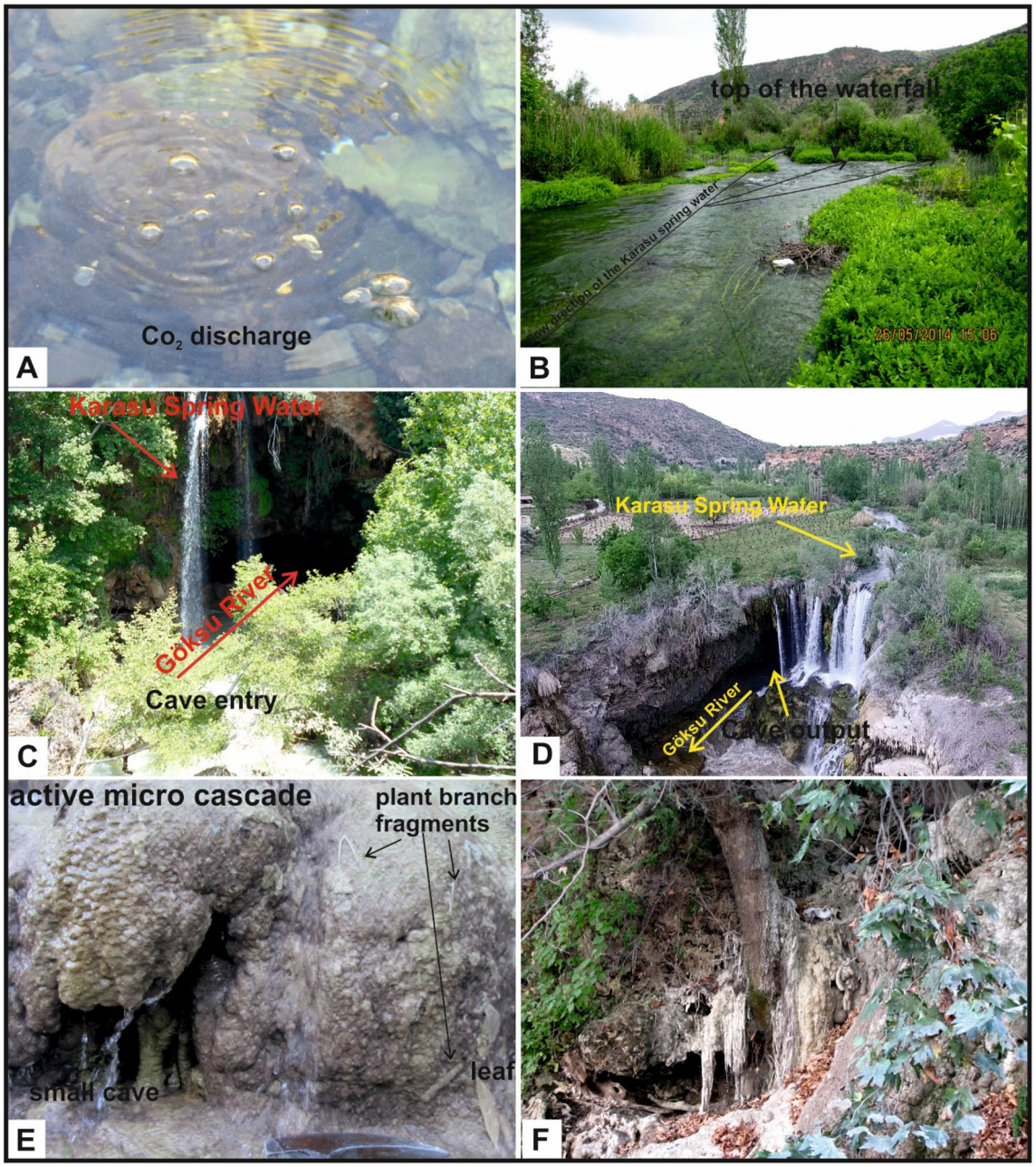

Fig. 4 **a** CO_2 degassing of bicarbonate-rich water of the Karasu spring. **b** Macrophytes in the Karasu spring water. **c** Cave entrances at the east side of Göksu River. **d** The waterfall of the Karasu spring and the output of the Göksu River from the cave. **e** Active micro-cascade environment. **f** Carbonate crust covering the roots of trees (facies Lvs)

channels as well as in fast-flowing channels (Pedley 1990; Ford and Pedley 1996; Sanders et al. 2011; Arenas and Jones. 2017). Stromatolitic tufa facies in the study area is deposited at the pond rims, flood plains, channels and cave walls (Figs. 3e, 5d, 7h and 8a–f). The alternation of light and dark lamina in this facies is interpreted as having resulted from seasonal changes and depositional rate (Pentecost and Whitton 2000; Andrews and Brasier 2005; Pedley 2009; Gradzinski 2010; Jones and Renaut 2010; Arp et al. 2010). The thick deposition in the watermill canal indicates fast sedimentation and resulted from fast-flowing water (Fig. 7g).

Micro detrital tufa facies (micritic tufa facies—Lm)

Description

This facies (Lm) is present within the recent and old pools on the natural bridge and the slopes of the valley near the

Table 1 Principal features and interpretation of tufa facies in the Yerköprü region (modified after Ford and Pedley 1996 and Vazquez-Urbez et al. 2012)

Facies		Geometry of deposits	Microstructure, textural features and components	Sedimentary structures	Identifiable biological content	Common associated facies	Depositional sedimentary context
Autochthonous tufa deposits							
Phytotherm framestone	Macrophytes—Lmp Vertical Stems—Lvs Bryophytes—Lbr	Lenticular, overhangs 10–300 cm, 5 m. İn lateral extent	Mainly laminated, coated perpendicular root, trunk and branches of trees cemented by calcite		Macrophytes and *Adiantum capillus-veneris* root and branches	Lbr, Ls, Lpc	Flood plane and cascade in fluvial setting
Phytotherm Boundstone	Stromatolitic tufa—Ls	Laminated calcite deposits, dome and hemi-dome shaped	Intercalated light and dark lamina, kidney and hemispheric-shaped structures. Thickness in the range of 30–60 cm	Horizontal and undulate lamination	Cyanobacteria and filamentous, *Diatom* sp. (Fig. 8)	Lmp, Lps, Lbr	Areas of slow-flowing to standing water such as pools and canal
Allochthonous tufa deposits							
Micro detrital tufa	Micrite tufa—Lm	Lenticular	Thick bedded lime mud	Horizontal bedding	Root, branches and plenty of leaves	Lbr, Lmp, Ls	Pool and flood plane
Macro detrital tufa	Phytoclastic tufa—Lpc	Lenticular, thick bedded	Angular grains bounded by lime mud	Horizontal bedding	Root, branches and plenty of leaves	Lbr, Lmp, Ls, Lvs	Pool and flood plane

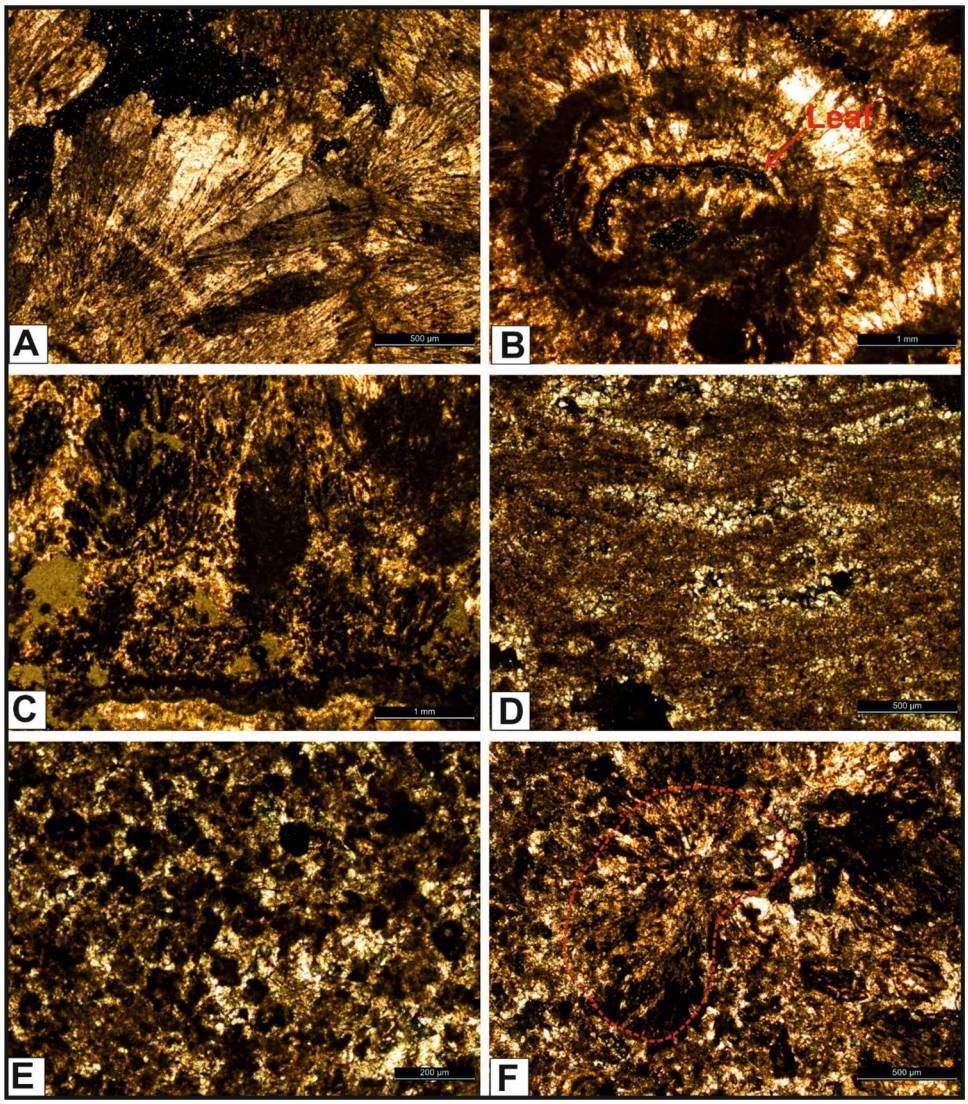

Fig. 5 **a** Low-Mg calcite developed as concentric rings around the tree roots (facies Lmp), **b** macrophyte facies formed by concentric micritic and sparitic rings encrusting around leaves. **c** Thin section appearance of bryophytes, **d** micritic lamina separated by coarse spray calcite (stromatolitic facies, Ls), **e** pelloidal facies (micritic tufa facies, Lm) deposited in small pools, **f** coarse radial calcite grows within the pelloidal facies

waterfall. It is represented by thick bedded lime mud deposited within these ponds and micro-pools (Figs. 5e, 9b). It contains voids that resulted from decaying of organic material. Some of these voids were filled with coarse aragonite crystals (Fig. 5f). Their thickness ranges from 10 to 83 cm. It has lenticular shape and rests conformably on the stromatolitic facies (Fig. 9a–c). Micritic sediments are generally surrounded by macrophyte tufa or stromatolites developed at the corner of the pools.

Interpretation

Micritic tufa facies has been interpreted as being deposited in quiet ponded areas by direct precipitation of fine calcite and/or fine particles derived from erosion of the surrounding and nearby facies (Ford and Pedley 1996; Arenas et al. 2007; Melón and Alonso-Zarza 2018).

Macro detrital tufa (phytoclastic tufa facies—Lpc)

Description

This facies consists of weakly consolidated fragments of highly variable size and shape (Fig. 9d). It is commonly associated with broken phytoclasts and stromatolites within the micrite matrix or spar cement. It has a thickness ranging from 15 to 48 cm and short lateral extension.

Interpretation

This facies was developed as channel fills and has lenticular shape. It contains mainly fragments of previously deposited facies, but the fragments of basement rocks and broken pottery are also present in lesser amounts. This facies represents the high discharging periods of the Karasu spring, causing flooding in the area, and originated from erosive processes

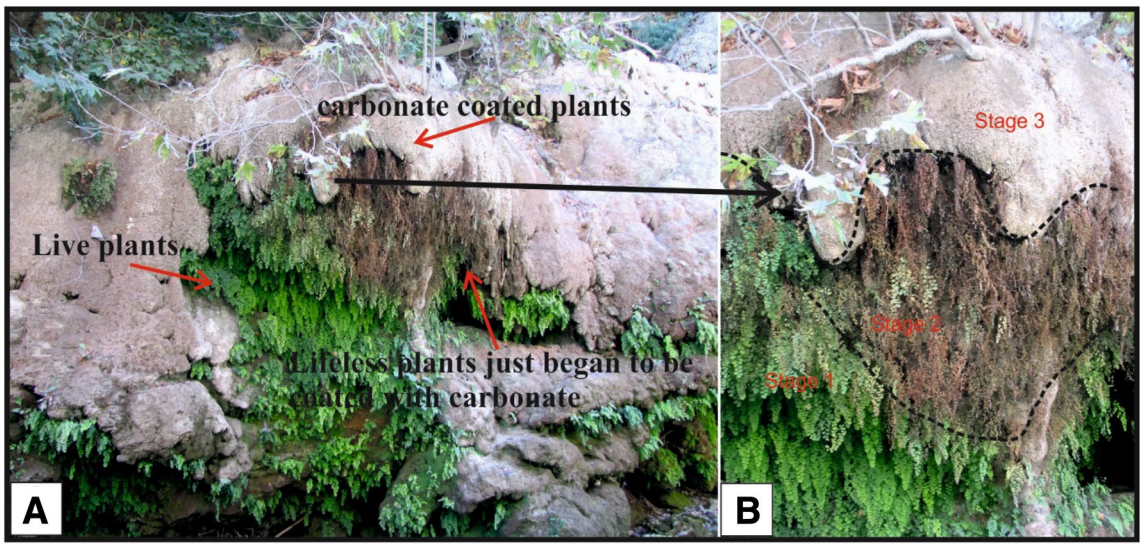

Fig. 6 Formation phases of the Lmp facies developed by downward vertical growing *Adiantum capillus-veneris* in cascade. **a** The three phases of crust development on living *Adiantum capillus-veneris* and caves behind them. **b** Umbrella looking Lmp facies developed at three phases

related to flooding events that affected previously deposited facies. Their thickness and extension are a function of the power and duration of the flooding.

Chemical composition of Karasu spring and Göksu River

Water samples collected from both the Göksu River and the Karasu spring were subjected to chemical analysis (Table 2). The bicarbonate ($H_2CO_3^{-1}$) contents of the Karasu spring water samples taken from the upstream, on and downstream of the waterfall were measured as 506,3 mg/L, 549 mg/L and 231,8 mg/L, respectively. On the other hand, the bicarbonate ($H_2CO_3^{-1}$) content of the Göksu River water taken before reaching the natural bridge was 131 mg/L. The pH of the water was slightly basic. The temperatures of the Göksu River and Karasu spring water were 20.3 °C and 16.5 °C, respectively (Table 2).

Geochemical composition of the tufa deposits

Mineralogical analysis indicates that all tufa samples are nearly pure calcite (Fig. 10). The element contents of tufa samples collected from different locations and facies are given in Table 3. The Mg content ranges from 2400 to 9780 with an average of 3786 ppm. The $MgCO_3$ of the tufa deposits ranges from 0.836 to 3.4067 mol% with an average of 1.3187 mol%, which indicates that tufa samples are composed of low magnesian calcite (Arenas et al. 2000; Ozkul et al. 2010). The Ba and Sr contents of the tufa samples were 31–61 ppm and 2384–4558 ppm, respectively. The Ba and Sr contents were slightly higher than those in the fluvio-lacustrine tufas in the central Ebro Depression, NE Spain (Arenas et al. 2000; Ozkul et al. 2010), while Ba content in the Quaternary tufa stromatolite from central Greece also had similar values (Andrews and Brasier 2005; Ozkul et al. 2010).

Stable isotope data

The $\delta^{13}C$ (V-PDB) and $\delta^{18}O$ (V-PDB) values were obtained mainly from recent phytotherm framestone facies. The $\delta^{13}C$ content of the tufa deposits ranged from 1,6 to −3,3 and $\delta^{18}O$ contents from −9,6 to −11,5 (Table 4). These values closely resemble the values obtained from fluvial tufa sediments in the Denizli-Sarıkavak region (Toker 2017).

Discussion

The field observation and chemical analysis of waters from the Karasu spring and the Göksu River showed clearly that the tufa deposition resulted only from the carbonate-rich water of the Karasu spring (Table 2). The water from Karasu spring flows on the natural bridge where the Göksu River flows beneath. The distance from the source of the Karasu spring to the waterfall is 700 m, but the tufa formation took place only on and around the waterfall where the water flow was fast and turbulent (Jet flow), causing aeration and low pressure on the carbonate-rich Karasu water. This increases the rate of degassing of CO_2. Tufa deposition in the waterfall area resulted from degassing of CO_2 due to sudden hydrological changes rather than due to the effects of organisms, evaporation and sediment–water interaction. This caused the

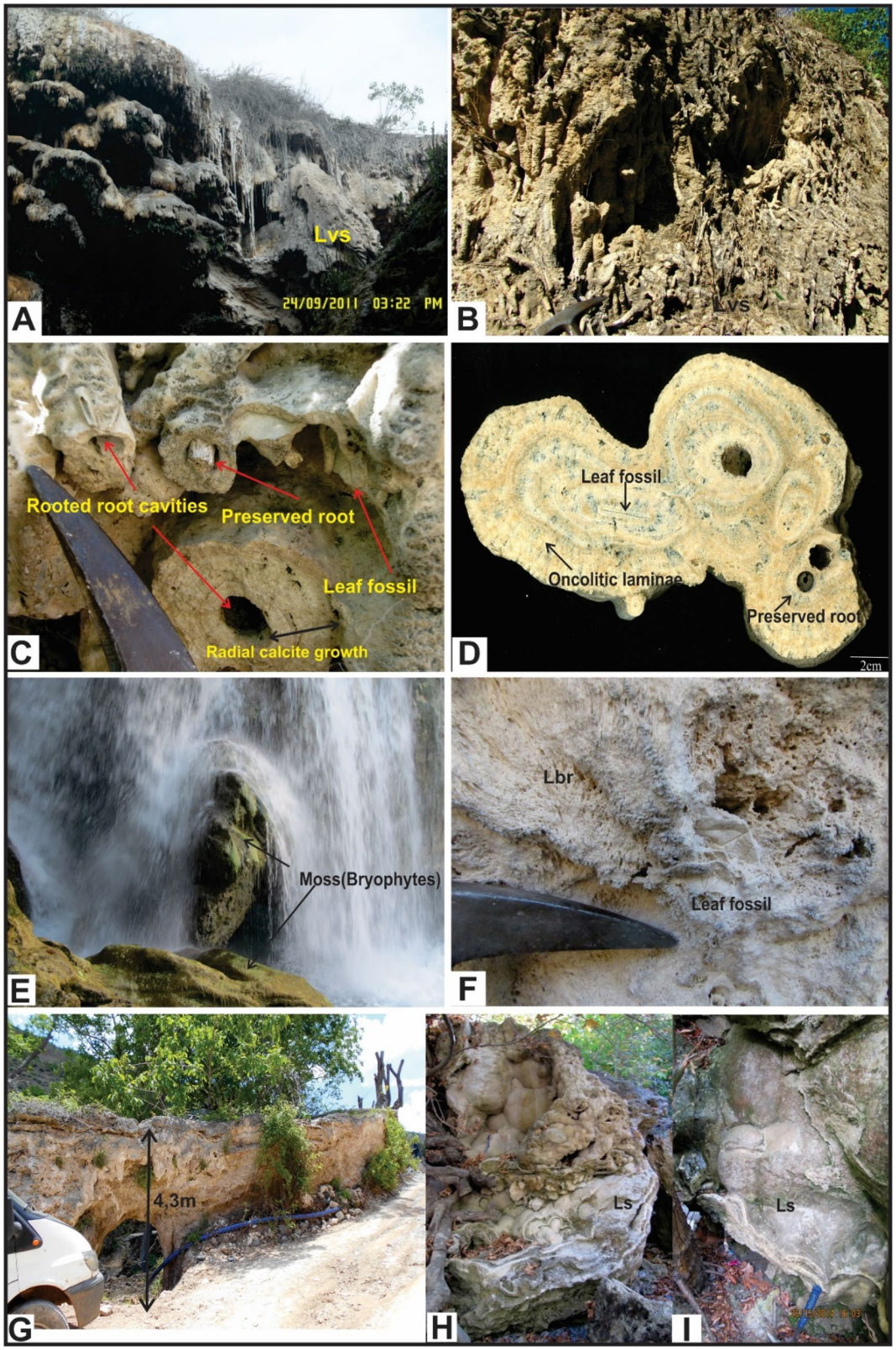

Fig. 7 Field photographs of the recent tufa. **a** Lmp facies formed on the vertical waterfalls with curtains of *Adiantum capillus-veneris*. **b** Detailed appearances of Lvs facies. **c** Tree roots coated by concentric rings (facies Lmp). **d** Radial aragonite overgrowths around the tree roots and leaves (polished section of facies Lmp). **e** Actual bryophytes growing on the tufa where the fast-moving water falls. **f** detailed view of bryophytes and leaves fossil. **g** Stromatolitic tufa deposits were formed in the watermill channels. **h**, **i** Stromatolite (facies Ls) with intercalated dark and light lamina

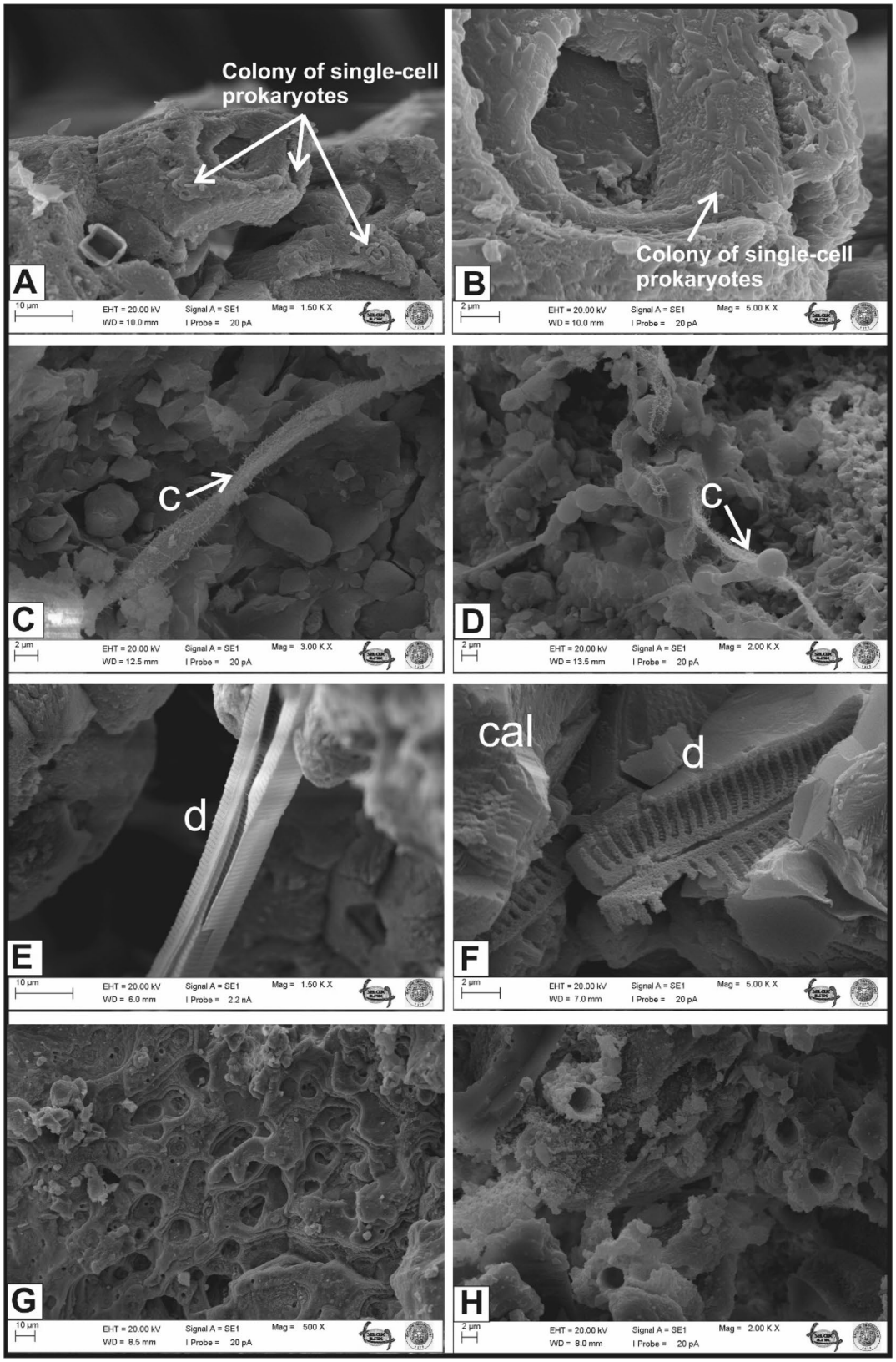

Fig. 8 Bacteria and fossils within the recent and old tufa sediments. **a**, **b** Single cell colonies; prokaryotes, **c**, **d** cyanobacteria filaments, **e**, **f** *Diatom* sp. and Cal: calcite crystals, **g**, **h** detailed view of moss facies

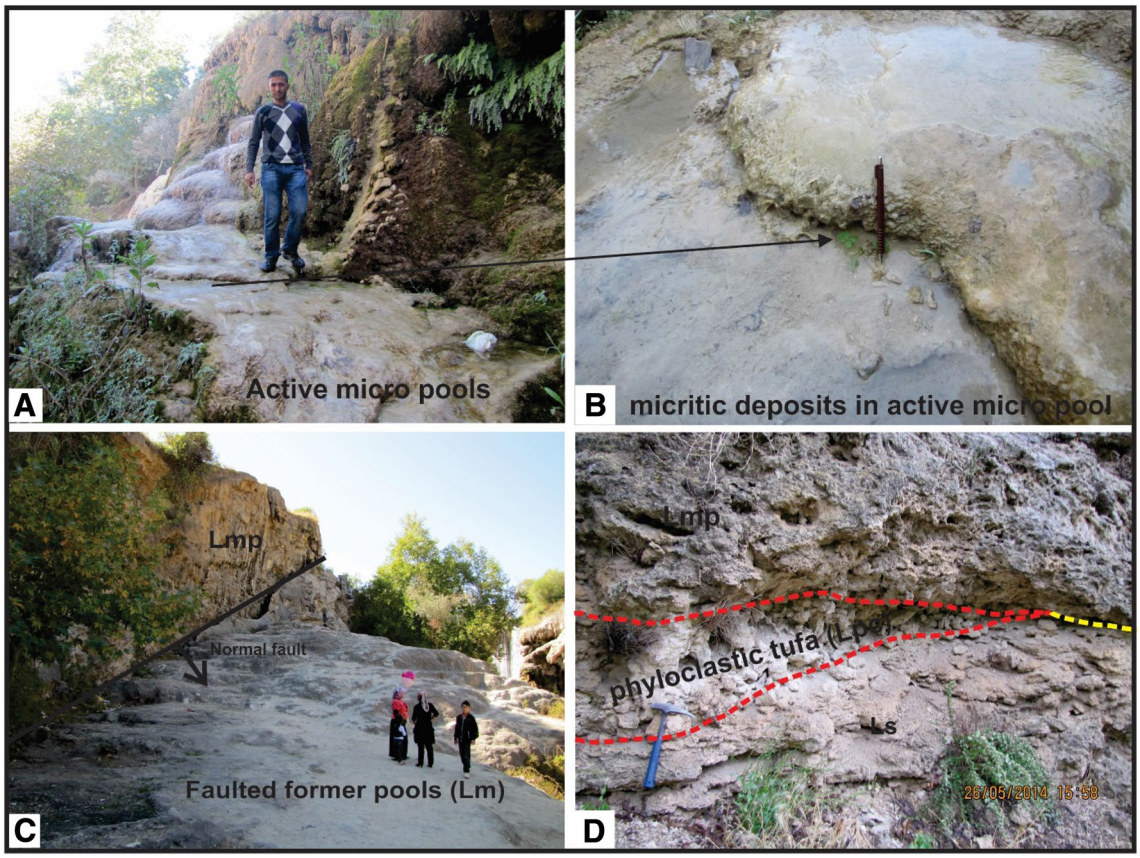

Fig. 9 Field views of tufa formation. **a** Micro-pools formed at the slopes and micritic carbonate deposition within them. **b** Close view of sediment in micro-pools (the pan is 14 cm.). **c** Sediment deposited within a large pool bordered by a fault just behind the slope. **d** Lenticular facies Lpc comprising fragments derived from facies Lmp during flooding

Table 2 Chemical composition of the Karasu spring water and the Göksu River

Measurement	Göksu River water (before waterfall)	Karasu spring water			
		Spring orifice	Waterfall top	Waterfall bottom (mixing zone)	Waterfall downstream Karasu and Göksu
Temperature (°C)	20.3	16.5	16.2	16.8	17.3
pH	7.90	6.98	7.38	7.79	7.67
Bicarbonate (mg/L)	131	506.3	549	244	231.8
Magnesium (mg/L)	6.22	25.51	33.05	11.18	9.48
Sodium (mg/L)	2.56	15.87	15.64	6.21	4.6
Potassium (mg/L)	0.745	3.12	3.12	1.17	1.17
Calcium (mg/L)	45.3	142.6	138.4	69.8	69
Sulfate (mg/L)	9.81	37.44	32.64	14.4	13.92
Chloride (mg/L)	4.01	24.11	25.17	11.34	10.64
Total alkalinity ($CaCO_3$) (mg/L)	120	415	450	200	190
Calcite saturation index (SIC)	0.20	0.18	0.59	0.45	0.32

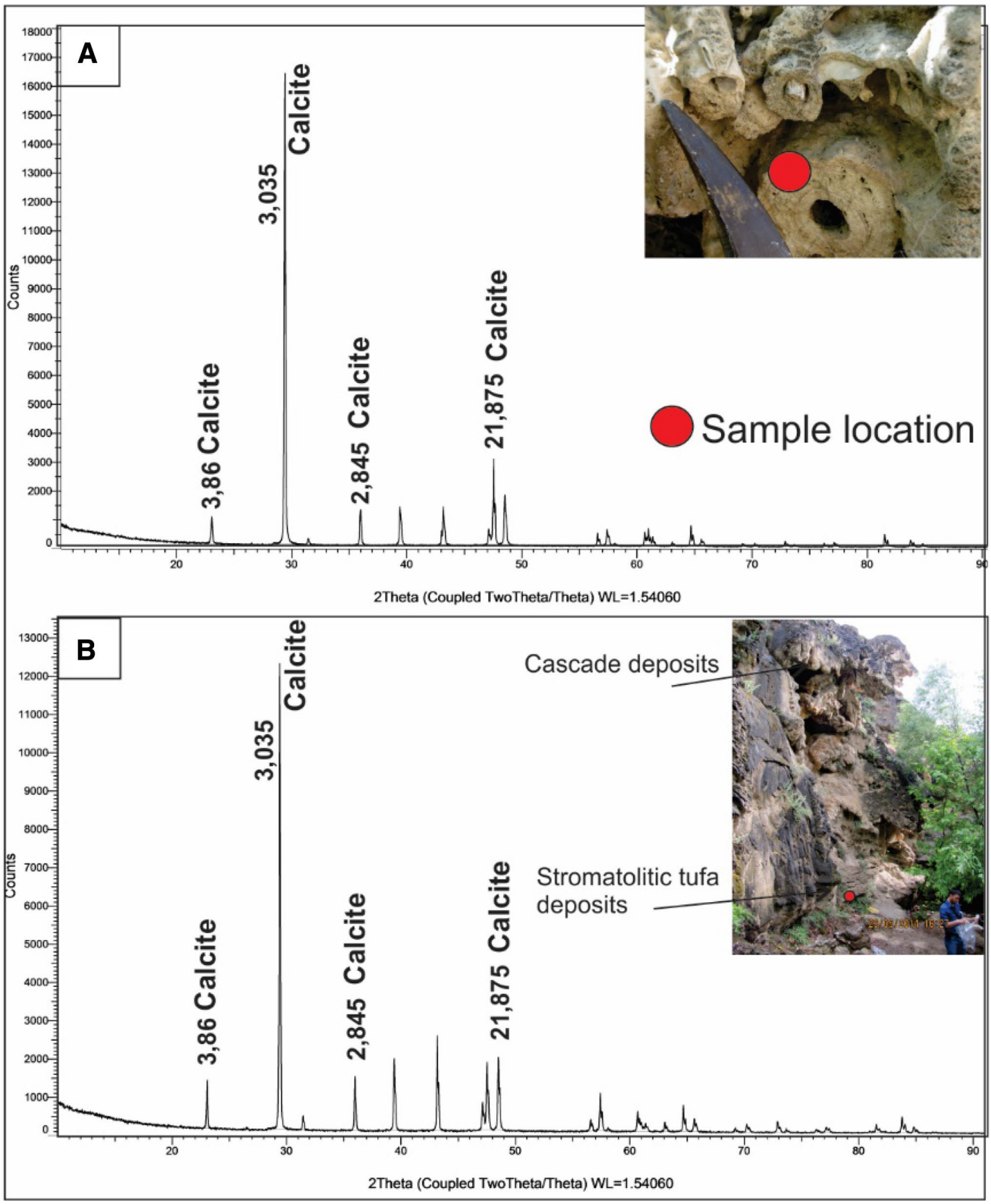

Fig. 10 The XRD diffractometry of the Lv facies (**a**) and the Ls facies (**b**) was generated by pure calcite

Table 3 Major and trace element contents (in ppm) and $MgCO_3$ contents (in mol%) of the Yerköprülü Tufa deposits

Sample	Si	Al	Fe	Mg	Ca	Sr	Ba	$MgCO_3$
9	5776.65	1134	572.4	4320	388.796	284.2	40	1.5048
14	16474.15	5481	1717.2	2460	3,88,086	406.8	61	0.8569
15	12,837	3591	1287.9	2760	3,91,778	300.3	40	0.9614
16	45357.4	14,364	4293	3660	3,78,998	291.5	52	1.2749
17	2567.4	189	572.4	4260	3,89,364	455.8	59	1.4839
18	7702.2	2079	715.5	2880	3,92,701	238.4	31	1.0032
19	11339.35	1323	572.4	9780	3,78,288	349.1	43	3.4067
21	5990.6	189	572.4	2760	3,94,902	412.4	59	0.9614
28D	8985.9	2457	858.6	2580	3,91,139	421.7	59	0.8987
29	2567.4	189	572.4	2400	3,94,192	395	51	0.836
Average	11959.81	3099.6	1173.42	3786	388824.4	355.52	49.5	1.31879

water to reach oversaturation and accelerate tufa deposition. This fast deposition of tufa on the waterfall is known as waterfall effect (aeration effect, low pressure effect and jet flow effect) (Zhang et al. 2001; Chen et al. 2004).

The rate of deposition depends on the seasonal changes and is greater during spring and summer (warm season, few cm/year) than during autumn and winter (cool season). The Karasu River flows in a relatively narrow channel (about 700 m) up to the waterfall area, where it branches out into small bars in a v-shape on the flat part of the natural bridge. Pools with various shapes and sizes developed as a result of spreading of water on the flatness close to the waterfall or redirection of the watercourse by humans. The facies Lm, Ls and Lmp were deposited within these pools. Water from pools and watercourse flows toward the waterfall or toward both sides of the Göksu River and mixes with the Göksu River. Tufa formation took place only on the Yerköprü natural bridge from the water of the Karasu spring. No tufa deposition site was observed on the upstream and downstream sites of the Göksu River.

Table 4 Stable isotope values of the Yerköprü tufa deposits

Sample	$\delta^{13}C$ (V-PDB)	$\delta^{18}O$ (V-PDB)	$\delta^{13}C_{CO2}$	Facies
10	0.6	−10.2	−9.78	Phytotherm framestone
11	0.5	−10.5	−9.9	Phytotherm framestone
12	0.6	−10.1	−9.78	Micritic tufa
13	−2.1	−10.2	−13.02	Phytotherm framestone
14	−0.3	−10.1	−10.86	Phytotherm framestone
15	0.2	−9.9	−10.26	Micritic tufa
16	0	−9.7	−10.5	Micritic tufa
17	1.6	−9.6	−8.58	Micritic tufa
18	0.1	−9.9	−10.38	Micritic tufa
19	−0.2	−10.1	−10.74	Phytotherm framestone
20	0	−9.6	−10.5	Phytotherm framestone
21	0	−10	−10.5	Phytotherm framestone
24	−0.6	−10.8	−11.22	Phytotherm framestone
25	−0.5	−10.5	−11.1	Phytotherm framestone
26	0.3	−10.2	−10.14	Phytotherm boundstone
27	0.1	−9.9	−10.38	Phytotherm framestone
28 L	−0.7	−10.7	−11.34	Phytotherm framestone
28 D	−0.4	−10.5	−10.98	Phytotherm boundstone
29	−0.2	−10	−10.74	Phytotherm framestone

Cascade formation took place by carbonate deposition in the micro-pools, at both sides of the waterfall and by carbonate coating of roots and branch of the trees (Figs. 3 and 6). Facies Lmp, Lbr and Lvs (Figs. 3d, 5a) were deposited in the cascade environment, and facies Lm and Ls in the micro-pools (Fig. 7a). Facies Lpc formed within the flooding channels and stromatolitic facies within small canals built for irrigation. The cascade sediments comprise calcite-coated moss mats at the vertical waterfall and various plants growing on the valley slope, stalactite and stalagmite in the cavities beneath the waterfall and stromatolitic tufa deposit on the damp walls of caves.

Cascade sediments formed as downward hanging masses often collapse due to their heavy weight. This sometimes changes the watercourse and causes the formation of different depositional settings (Fig. 9c). The collapsed bodies are often covered by new tufa deposits which are mainly controlled by the size and shape of the collapsed body and the vegetation covers growing on them.

Tufa-depositing spring waters emerging from karstic massifs are commonly of the $Ca–HCO_3$ and $Ca–HCO_3–SO_4$ types and are supersaturated with respect to calcite (Ozdemir and Nalbantcilar 2002; Ozkul et al. 2010, Khalaf 2017; Nicoll and Sallam 2017). Calcium and bicarbonate are the dominant ions in the Karasu spring water (Table 2). Therefore, the water of Karasu spring is classified as a $Ca–HCO_3$ type.

Field observations show that tufa sediments are only deposited on the pathway of the Karasu spring. No tufa sedimentation has been observed along the Göksu River itself. The $H_2CO_3^{-1}$ content of the water sample taken from the orifice of

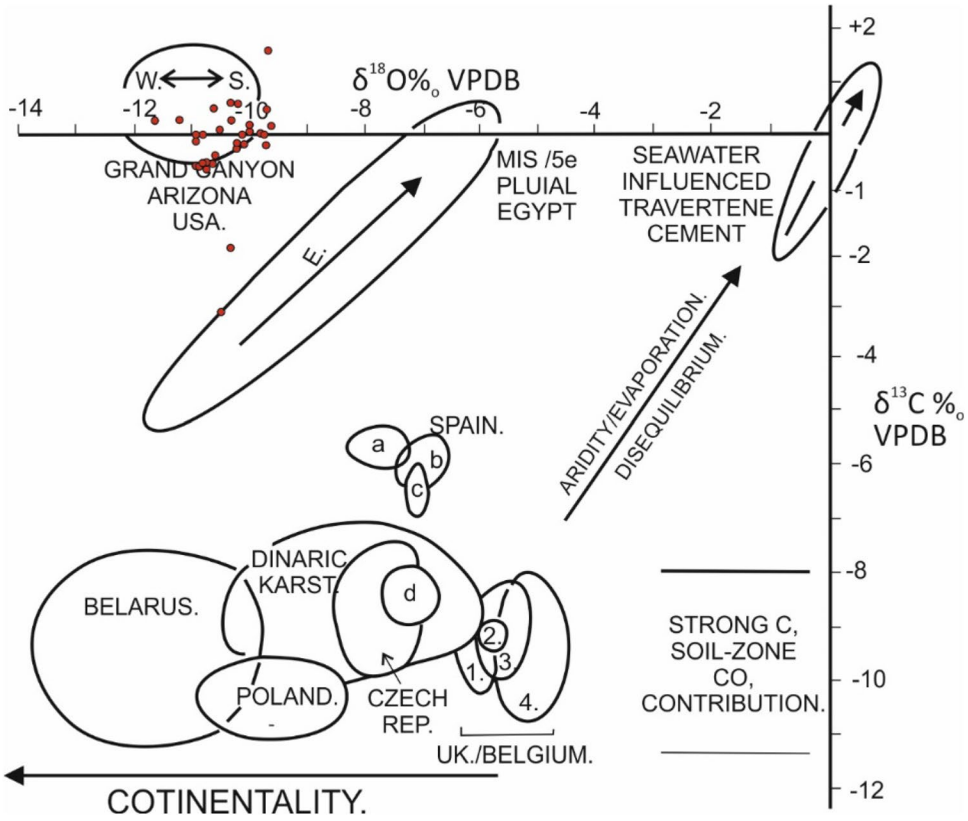

Fig. 11 The distribution $\delta^{18}O$ and $\delta^{13}C$ valoes of the Yerköprü tufa deposits on the plot introduced by Andrews (2006)

the Karasu spring, where the degassing of CO_2 starts (Fig. 4a), is 5063 mg/L. But it was measured as 549 mg/L at the edge of the waterfall and as 2318 mg/L at the base of the waterfall where the water mixes with the Göksu River. The distance between the orifice and the waterfall edge is 700 m.

The calcite saturation indices (SIC) is 0,18 at the orifice, 0,59 on the top of the waterfall and 0,45 at the bottom of the

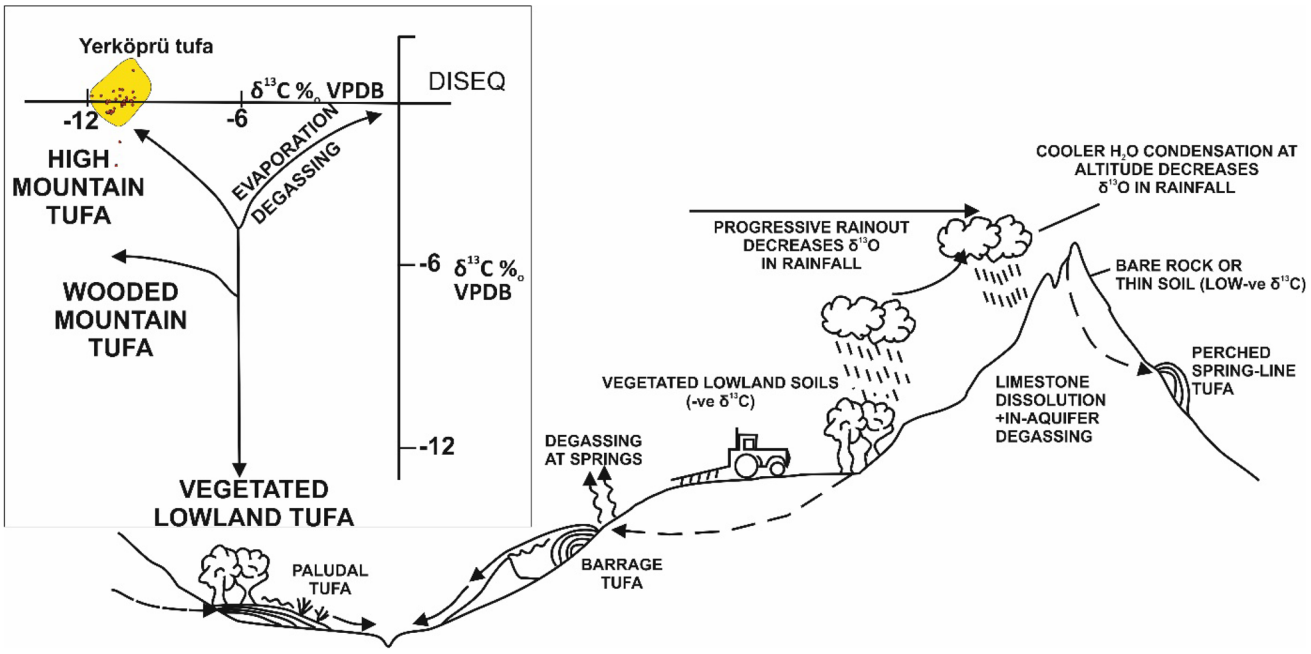

Fig. 12 Regional setting of the Yerköprü tufa deposits based on the $\delta^{18}O$ and $\delta^{13}C$ stable isotope data plot of Andrews (2006). The tufa deposits in this study correspond to 'high mountain tufa'. See for details Andrews (2006)

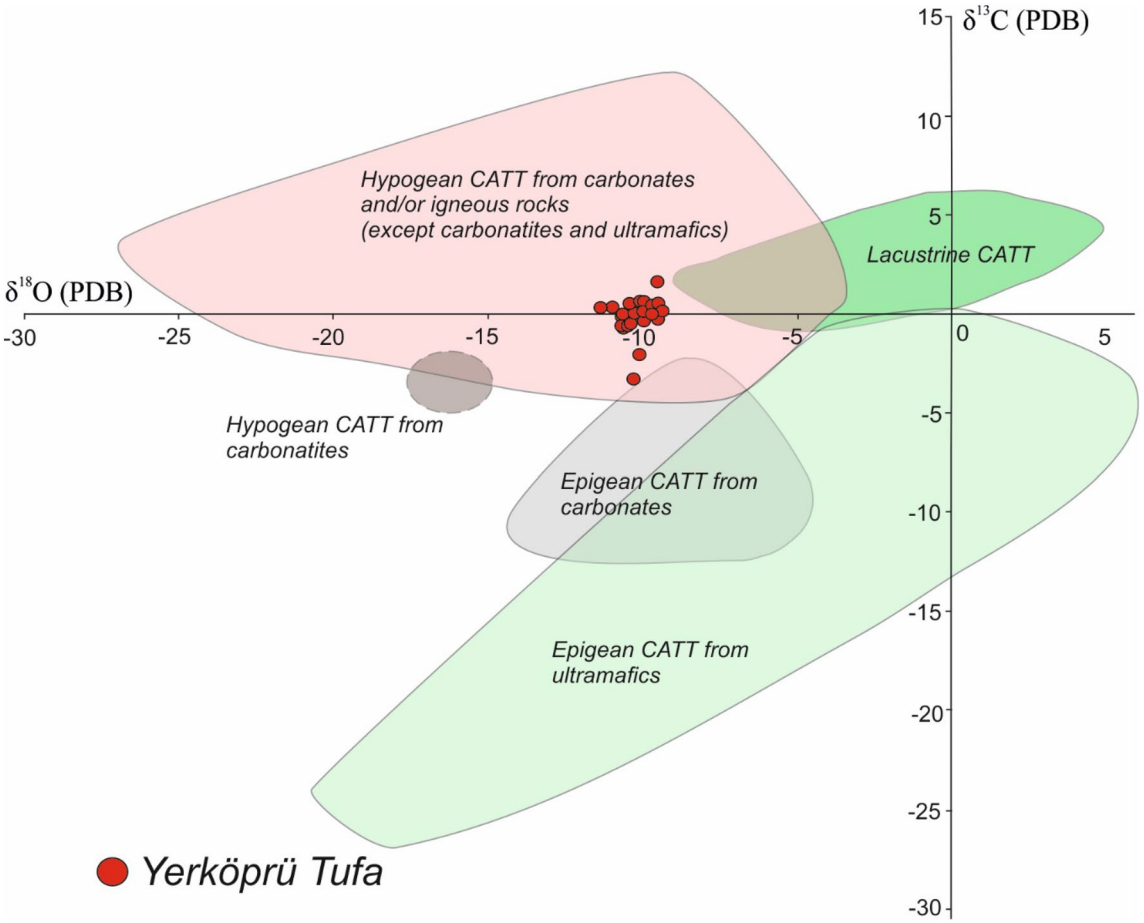

Fig. 13 The distribution of $\delta^{18}O$ and $\delta^{13}C$ values of the studied samples on the combined $\delta^{18}O$ (‰PDB) and $\delta^{13}C$ (‰PDB) plot for recent to modern calcitic or aragonitic travertine and tufa (CATT; Teboul et al. 2016)

waterfall (Table 2). It is minimum at the orifice, but decreases rapidly along the flow path due to CO_2 degassing and reaches the maximum at the top of the waterfall where dense tufa deposition has taken place.

The $\delta^{18}O$ and $\delta^{13}C$ values obtained from the studied tufa samples, which is located at about 725 m altitude, resemble those from the tufa deposits in the Grand Canyon, Arizona, USA (Fig. 11; Andrews 2006) and fall in the 'High mountain tufa' area on the plot (Fig. 12) constructed by Andrews (2006). "High mountain tufa" represents the tufa deposition from the karstic water flowing out along a fracture in a high-altitude (700–800 m) setting (perched springline tufa, Andrews 2006). The characteristics of the studied tufa deposits such as the altitude (725 m) and source of carbonate-rich waters (the dissolution of older carbonate rocks) correspond exactly to the descriptions by Andrews (2006). The interpretation introduced by Teboul et al. (2016) also supports the idea that the bicarbonate in the Karasu water was derived from dissolution of older carbonate rocks (Fig. 13).

The stable isotope values of the tufa deposits are controlled by different parameters such as biological activities, evaporation, water temperature, turbidity, bed configuration and altitude (O'Brien et al. 2006; Gandin and Capezzuoli 2008; Arenas-Abad et al. 2010; Hassan 2014; Toker 2017). The $\delta^{18}O$ values (−9.6 to −11.5) of the tufa sediment in the studied area resemble those of many other places (Vazquez-Urbez et al. 2012; Arenas et al. 2000, 2007; Zamarreno et al. 1997, Ozkul et al. 2010; Kosun 2012; Orhan and Kalan 2015; Toker 2017), while the $\delta^{13}C$ values are much higher (1.6 to −3.3). These high values of $\delta^{13}C$ point to the dissolution of the carbonate aquifer (Andrews et al. 1993). As can be seen in Fig. 14, the isotopic values of the tufa samples fall in the travertine area. The field measurements show that the Yerköprü tufa sediments were deposited from cold water. The carbonate-rich water derived from dissolution of carbonate aquifer has the hydrochemical signals of deep circulation, which is similar to the tufa formation "travitufa" in a specific setting (Capezzuoli et al. 2014; Toker 2017). The drop in $\delta^{18}O$ is related to the decrease in temperature and prevalence of the freshwater, which can be seen clearly in the Yerköprü tufa deposits (Andrews 2006; Toker 2017).

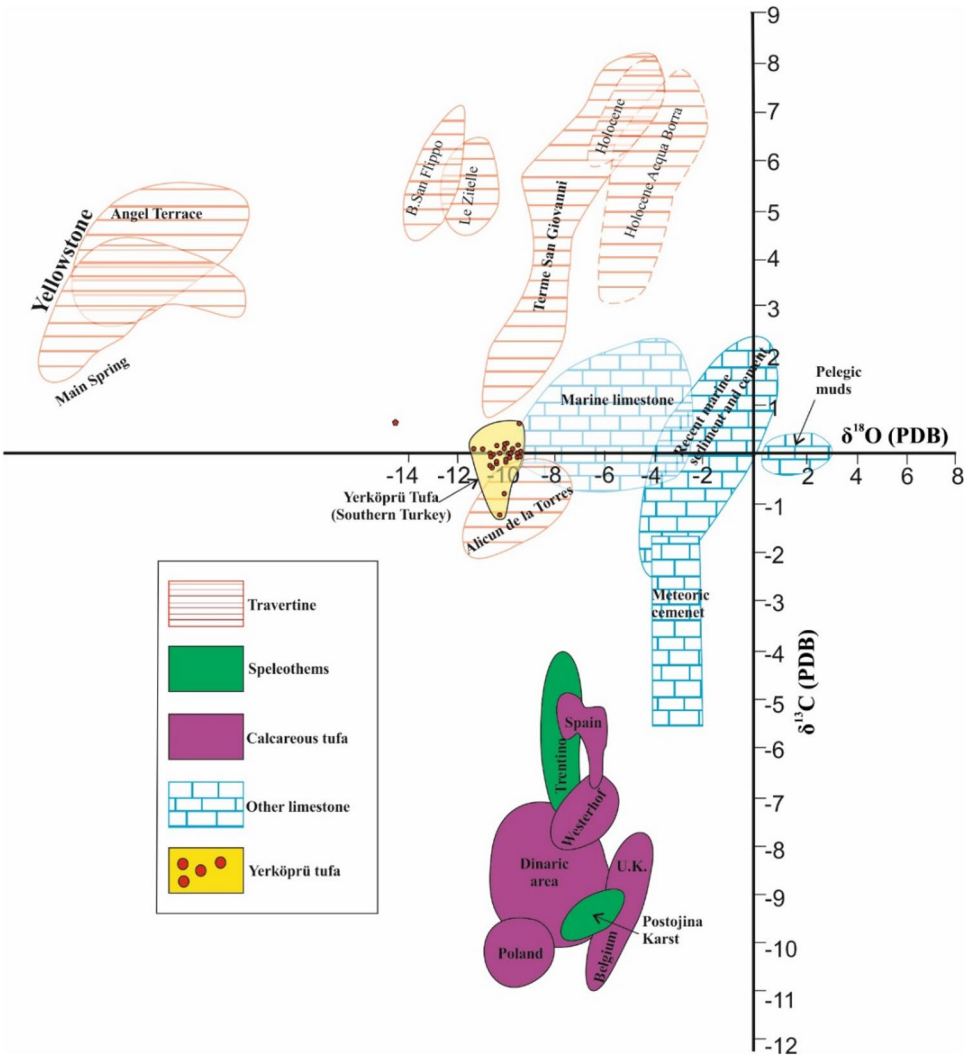

Fig. 14 Combined plot of $\delta^{18}O$ (‰PDB) and $\delta^{13}C$ (‰PDB) values derived from carbonates presently forming in terrestrial (travertine, calcareous tufa, speleothems) and marine (skeletal-ooid sediments and pelagic muds) environments and from lithified marine limestones (Gandin and Capezzuoli 2008)

Conclusion

This is a first study on the sedimentological and geochemical characteristics of the recent tufa deposits in the study area which is tectonically active. The following conclusions were introduced after evaluating field, sedimentological and geochemical data.

1. The field observation and chemical analysis data showed that the tufa deposition resulted from the carbonate-rich water of the Karasu spring.
2. Based on the thickness data obtained from the deposition in an artificial canal in the area, the tufa sedimentation rate is at least 1 cm/year.
3. The Yerköprü tufa deposition took place in a small graben as a natural bridge, which is a rare structure. Its formation in the area is related to the neotectonic activities. Therefore, the deposition is topographically controlled.
4. There is an active cascade formation in the study area. Even though most of the tufa deposition took place in the cascade setting, some deposits were in small lakes and ponds around the waterfall. Fluvial deposits occur as lenticular phytoclast sediment. Except for the fluvial and oncolitic facies, other representative facies (Lmp, Lvs, Lbr, Ls, Lm, Lpc; see Table 1). are present in the studied area.
5. The $\delta^{18}O$ and $\delta^{13}C$ values of the Yerköprü tufa sediments is classified as "High mountain tufa" of Andrews (2006) which was deposited from karstic water discharging on a fracture. The high $\delta^{13}C$ values (1.6 to −3.3) of tufa sediments in the Yerköprü area show that the bicarbonate in the Karasu spring was derived from the dissolution in the carbonate rocks.
6. The isotopic values of the studied tufa samples fall in the travertine area in Fig. 14, but the Karasu water is interpreted as cold water. Therefore, it can be classified as "travitufa".

Acknowledgements This work was supported by the Selcuk University Scientific Research Fund (BAP, Project Number: 11201066). This article was produced from the master thesis of Mehmet Mert, supervised by Arif Delikan We thank Prof. Dr. Hükmü Orhan for constructive comments that improved the manuscript. We also thank the anonymous reviewers for their valuable comments.

References

Andrews JE (2006) Paleoclimatic records from stable isotopes in riverine tufas; synthesis and review. Earth Sci Rev 75:85–104

Andrews JE, Brasier AT (2005) Seasonal records of climate change in annually laminated tufas: short review and future prospects. J Quat Sci 20:411–421

Andrews JE, Riding R, Dennis PF (1993) Stable isotopic compositions of recent cyanobacterial carbonates from the British Isles: local and regional environmental controls. Sedimentology 40:303–314

Arenas C, Jones B (2017) Temporal and environmental significance of microbial lamination: insights from Recent fluvial stromatolites in the River Piedra, Spain. Sedimentology 64:1597–1629

Arenas C, Gutierrez F, Osacar C, Sancho C (2000) Sedimentology and geochemistry of fluvio-lacustrine tufa deposits controlled by evaporite solution subsidence in the central Ebro Depression, NE Spain. Sedimentology 47:883–909

Arenas C, Cabrera L, Ramos E (2007) Sedimentology of tufa facies and continental microbialites from the Paleogene of Mallorca Island (Spain). Sed Geol 197:1–27

Arenas C, Azquez-Urbez M, Pardo G, Sancho C (2014) Sedimentology and depositional architecture of tufas deposited in stepped fluvial systems of changing slope: lessons from the Quaternary Añamaza valley (Iberian Range, Spain). Sedimentology 61:133–171

Arenas-Abad C, Vazquez-Urbez M, Pardo-Tirapu G, Sancho-Marcen C (2010) Fluvial and associated carbonate deposits. In: Alonso-Zarza AM, Tanner LH (eds) Developments in sedimentology: carbonates in continental settings: facies, environments and processes. Elsevier, Amsterdam, pp 133–175

Arp G, Bissett A, Brinkmann A, Cousin S, De Beer D, Fried T, Mohr KI, Neu TR, Reimer A, Shiraishi F, Stackebrandt E, Zippel B (2010) Tufa-forming biofilms of German karst water streams: microorganisms, exopolymers, hydrochemistry and calcification. In: Pedley HM, Rogerson M (eds) Tufas and speleothems: unravelling the microbial and physical controls, vol 336. Geological Society, London, pp 83–118

Baker A, Smart PL, Ford DC (1993) Northwest European paleoclimate as indicated by growth frequency variations of secondary calcite deposits. Paleogeogr Paleoclimatol Paleoecol 100:291e301

Brasier AT, Andrews JE, Kendall AC (2011) Diagenesis or dire genesis? The origin of columnar spar in tufa stromatolites of central Greece and the role of chironomid larvae. Sedimentology 58:1283–1302

Capezzuoli E, Gandin A, Pedley M (2014) Decoding tufa and travertine (fresh water carbonates) in the sedimentary record: the state of the art. Sedimentology 61:1–21

Chen J, Zhang DD, Wang S, Xiao T, Huang R (2004) Factors controlling tufa deposition in natural waters at waterfall sites. Sed Geol 166:353–366

Delikan A, Mert M (2014) Depositional properties of geomorphologically controlled Holocene tufas in a valley from Hadim-Yerköprü (Konya-Southern Turkey). GeoFrankfurt 2014 Earth System Dynamics, Abstract Volume Page, 38, Frankfurt-Germany

Delikan A, Orhan H, Ekici G, Sayin U, Ozmen A (2017) Yerköprü (Hadim-Konya) bölgesinde tufa çökellerinin ESR metodu ile yaşlandirilabilirliği hakkında ilk bulgular. Sedimantoloji Çalışma Grubu 2017 Çalıştayı (Karasal Çökelme Sistemleri), Abstract Book, p. 76, Rize-Turkey

Della Porta G (2015) Carbonate build-ups in lacustrine, hydrothermal and fluvial settings: comparing depositional geometry, fabric types and geochemical signature. Microbial carbonates in space and time: implications for global exploration and production, vol 418. Geological Society, London

Domínguez-Villar D, Vazquez-Navarro JA, Cheng H, Edwards RL (2011) Freshwater tufa record from Spain supports evidence for the past interglacial being wetter than the Holocene in the Mediterranean region. Global Planet Change 77:129–141

Ford TD, Pedley HM (1996) A review of tufa and travertine deposits of the world. Earth Sci Rev 41:117–175

Gandin A, Capezzuoli E (2008) Travertine versus calcareous tufa: distinctive petrologic features and stable isotopes signatures. Ital J Quat Sci 21:125–136

Glover C, Robertson AHF (2003) Origin of tufa (cool-water carbonate) and related terraces in the Antalya area, SW Turkey. Geol J 38:329–358

Gradzinski M (2010) Factors controlling growth of modern tufa: results of a field experiment. Geol Soc Spec Pub 336:143–191

Guo L, Riding R (1998) Hot-spring travertine facies and sequences, Late Pleistocene Rapolano Terme, Italy. Sedimentology 45:163–180

Guo L, Riding R (1999) Rapid facies changes in Holocene fissure ridge hot spring travertines, Rapolano Terme, Italy. Sedimentology 46:1145–1158

Hancock PL, Chalmers RML, Altunel EC, Akır Z (1999) Travitonics: using travertines in active fault studies. J Struct Geol 21:903–916

Hassan KM (2014) Note on the isotopic geochemistry of fossil-lacustrine tufas in carbonate plateau: a study from Dungul region (SW Egypt). Chem Erde 74:285–291

Henchiri M (2014a) Quaternary paludal tufas from the Ben Younes spring system, Gafsa, southwestern Tunisia: interactions between tectonics and climate. Quat Int 338:71–87

Henchiri M (2014b) Sedimentology of Quaternary calcareous tufas from Gafsa, southwestern Tunisia. Arab J Geosci 7(5):2081–2209

Henning GJ, Grun R, Brunnacker K (1983) Speleothems, travertines and paleoclimates. Quat Res 20:1229

Jones B, Renaut R (2010) Calcareous spring deposits in continental settings. In: Alonso-Zarza AM, Tanner LH (eds) Continental settings: facies, environments and processes., pp 177–224

Karaisaoğlu S, Orhan H (2018) Sedimentology and geochemistry of the Kavakköy travertine (Konya, central Turkey). Carbonates Evaporites. https://doi.org/10.1007/s13146-018-0436-z

Khalaf FI (2017) Occurrence and genesis of Quaternary microbialitic tufa at Hammam Al Ali, Oman. J Afr Earth Sci 129:417–426

Kosun E (2012) Facies characteristics and depositional environments of Quaternary tufa deposits, Antalya, SW Turkey. Carbonate Evaporites 27:269–289

Magnin F, Guendon JL, Vaudour J, Martin P (1991) Les travertins: accumulations carbonate Esassociees aux systemes karstiques sequences sedimentaires et paleoenvironnements quaternaries. Bull Soc Geol Fr 162(3):585–594

Martìn-Algarra A, Martìn-Martìn M, Andreo B, Juliá R, González-Gómez C (2003) Sedimentary patterns in perched spring travertines near Granada (Spain) as indicators of the palaeohydrological and palaeoclimatological evolution of a karst massif. Sed Geol 161:217–228

Melón P, Alonso-Zarza AM (2018) The Villaviciosa tufa: a scale model for an active cool water tufa system, Guadalajara (Spain). Facies 64:5

Nicoll K, Sallam ES (2017) Paleospring tufa deposition in the Kurkur Oasis region and implications for tributary integration with the River Nile in southern Egypt. J Afr Earth Sci 136:239–251

O'Brien GR, Kaufman DS, Sharp WD, Atudorei V, Parnell RA, Crossey LJ (2006) Oxygen isotope composition of annually banded modern and mid- Holocene travertine and evidence of paleomonsoon floods, Grand Canyon, Arizona, USA. Quat Res 65:366–379

Orhan H, Kalan F (2015) Sedimentological characteristic of Quaternary Aydıncık tufa (Mersin-Türkiye). Carbonates Evaporites 30:451–459

Ozdemir A, Nalbantcilar MT (2002) The investigation of mass transfer in the Karasu karstic aquifer, Konya, Turkey. Hydrogeol J 10:656–661

Ozkul M, Gokgoz A, Horvatincic N (2010) Depositional properties and geochemistry of Holocene perched springline tufa deposits and associated spring waters: a case study from the Denizli province, Western Turkey. In: Pedley HM (ed) Tufas and speleothems: unravelling the microbial and physical controls, vol 336. The Geological Society, London, pp 245–262

Özkul M, Gökgöz A, Sandor K, Baykara MO, Shen CC, Chang YW, Kaya A, Hançer M, Aratman C, Taylan A, Örü Z (2014) Sedimentological and geochemical characteristics of a fluvial travertine: a case from the eastern Mediterranean region. Sedimentology 61:291–318

Pedley HM (1990) Classification and environmental models of cool freshwater tufas. Sed Geol 68:143–154

Pedley HM (2009) Tufas and travertines of the Mediterranean region: a testing ground for freshwater carbonate concepts and developments. Sedimentology 56:221–246

Pedley M, Andrews J, Ordonez S, García del Cura MA, Gonzolez Martín JA, Taylor D (1996) Does climate control the morphological fabric of freshwater carbonates? A comparative study of Holocene barrage tufas from Spain and Britain. Paleogeogr Paleoclimatol Paleoecol 121:239–257

Pedley M, Gonzalez Martín JA, Ordonez S, García del Cura MA (2003) Sedimentology of Quaternary perched springline and paludal tufas: criteria for recognition, with examples from Guadalajara Province, Spain. Sedimentology 50:23–44

Peng X, Jones B (2013) Patterns of biomediated $CaCO_3$ crystal bushes in hot spring deposits. Sediment Geol 294:105–117

Pentecost A (2005) Travertine. Springer, Berlin, p 445

Pentecost A, Viles HA (1994) A review and reassessment of travertine classification. Geogr Phys Quat 48:305–314

Pentecost A, Whitton BA (2000) Limestones. In: Whitton BA, Potts M (eds) The ecology of cyanobacteria. Kluwer, Amsterdam, pp 257–279

Pisciotta A, Tiwari AK, De Maio M (2018) An integrated multivariate statistical analysis and hydrogeochemical approaches to identify the major factors governing the chemistry of water resources in a mountain region of northwest Italy. Carbonates Evaporites. https://doi.org/10.1007/s13146-018-0452-z

Pla-Pueyo S, Viseras C, Henares S, Yeste M, Candy I (2017) Facies architecture, geochemistry and paleoenvironmental reconstruction of a barrage tufa reservoir analog (Betic Cordillera, S. Spain). Quat Int 437:15–36

Richter DK, Immenhauser A, Neuser RD, Mangin A (2015) Radiaxial-fibrous and fascicular-optic Mg-calcitic cave cements: a characterization using electron backscattered diffraction (EBSD). Int J Speleol 44:91–98

Sancho C, Arenas C, Vázquez-Urbez M, Pardo G, Lozano MV, Peña-Monné JL, Hellstrom J, Ortiz JE, Osácar MC, Auqué L, Torres T (2015) Climatic implications of the Quaternary fluvial tufa record in the NE Iberian Peninsula over the last 500 ka. Quat Res 84:398–414

Sanders D, Wertl W, Rott E (2011) Spring-associated limestones of the Eastern Alps: overview of facies, deposystems, minerals, and biota. Facies 57:395–416

Teboul PA, Durlet C, Gaucher EC, Virgone A, Girard JP, Curie J, Lopez B (2016) Origins of elements building travertine and tufa: new perspectives provided by isotopic and geochemical tracers. Sed Geol 334:97–114

Toker E (2017) Quaternary fluvial tufas of Sarıkavak area, southwestern Turkey: facies and depositional systems. Quat Int 437:37–50

Vazquez-Urbez M, Arenas C, Pardo G (2012) A sedimentary facies model for stepped, fluvial tufa systems in the Iberian Range (Spain): the Quaternary Piedra and Mesa valleys. Sedimentology 59:502–526

Zamarreno I, Anadon P, Utrilla R (1997) Sedimentology and isotopic composition of Upper Paleocene to Eocene non-marine stromatolites, eastern Ebro Basin, NE Spain. Sedimentology 44:159–176

Zhang DD, Zhang Y, Zhu A, Cheng X (2001) Physical mechanisms of river waterfall tufa (travertine) formation. J Sediment Res 71:205–216